EWEA 2016 Annual Conference - Abstract

Influence of tip speed ratio on a real wind turbine wake profile using LiDAR

Satoshi Nakashima*, Hiroaki Fujio, Nobutoshi Nishio, Chuichi Arakawa, Makoto Iida**

Satoshi Nakashima, Hiroaki Fujio, Chuichi Arakawa and Makoto Iida, The University of Tokyo, 7-3-1 Hongo, Bunkyo-ku, Tokyo, Japan
Nobutoshi Nishio, Electric Power Development Co., Ltd., 6-15-1 Ginza, Chuoku-ku, Tokyo, Japan

Key Words: Wind Turbine, Wake, Field Test, LiDAR, Tip speed ratio

1. Introduction

Wind turbines arranged in a wind farm is an efficient form of wind turbine operation from a profitability viewpoint; however, when a wind turbine operates in the wake of an upstream turbine, it produces less power than it does in a free stream. The properties of a wind turbine wake depend on many factors such as wind conditions, wind turbine operating conditions and yaw angle [1]–[3]. Previous studies of wind tunnel tests showed that the turbulence intensity in the freestream affects the downstream recovery of the velocity deficit in the wake [4], and a field test found that the velocity deficit in the wake recovers more rapidly in a field than in a wind tunnel [5]. Some research studies reported the influences of tip speed ratio and yaw angle on wind turbine wake [3], [6], [7]. In these wind tunnel tests, hot-wire anemometer, pitot-static probe, Laser Doppler Anemometer and particle image velocimetry were used for the wake measurements; however, these devices are not available for some MW-turbine-scale wake measurements. In addition, common measurements for actual-turbine-scale using sonic anemometers and cup anemometers set up on a turbine nacelle or a met mast are point observation devices and are not suitable for actual-scale wake measurements.

Light Detection and Ranging (LiDAR) is one of the devices used for field measurements of the wake produced by real wind turbines. LiDAR can measure wind flows over a wide range and at high altitude with high resolution. Gallacher and More used LiDAR to measure the wake of a wind turbine in order to investigate the wake decay length, and they compared the PARK wake model with the measured data using LiDAR to assess its effectiveness in wake modelling [8]. Another set of field measurements of wake using two LiDARs was performed by Iungo et al.; their study showed that the mean vertical velocity is practically negligible for all the considered downstream locations [9].

In order to settle the appropriate turbine-setting distance, wake models that assess interactions between turbines are required; however, there is currently no general-purpose wake model. Therefore, data storage of field measurements is necessary for the development of general-purpose wake model of real turbines. Especially in Japan, it is important to investigate the effects of terrain configuration, with a high turbulence intensity found in complex terrains and mountainous terrains. It is also important to study the influences of the wind turbine operation conditions on the wake characteristics of real turbines.

The aim of this paper is to store the data obtained from field tests for the development of real-scale wake models that include the influences of the operation of wind turbines on the wake by investigating the effects of tip speed ratio on the real-scale wake characteristics via measurements of the wake of a real wind turbine at a flat terrain using LiDAR.

*Presenting author. **Corresponding author.
E-mail:
nakashima.satoshi@gg.cfdl.t.u-tokyo.ac.jp (Satoshi Nakashima)
iida@ilab.eco.rcast.u-tokyo.ac.jp (Makoto Iida)

2. Approach

The LiDAR field test was performed at a flat terrain site in Japan in July and August 2015; Figure 1 shows the general view of the field test site. The wind turbine was located near the shore line.

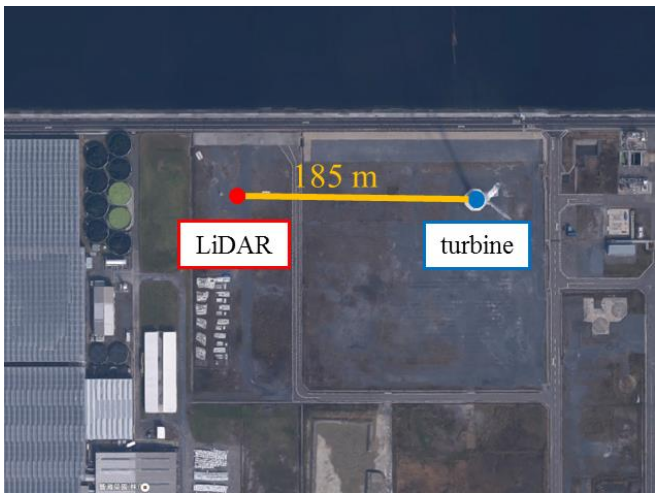

Figure 1: Overview of the field test site

Table 1 shows the major specifications for the wind turbine. Sonic anemometers and wind vanes were set up on the turbine nacelle.

Table 1: Wind turbine specifications

Rated power	2,700 kW
Rotor diameter	103.4 m
Hub height	80 m
Rated Wind Speed	13 m/s
Cut-in wind speed	4.0 m/s
Type	Horizontal axis (upwind)

Galion, provided by Japan Meteorological Corporation, was used for the LiDAR measurements. The major specifications for the LiDAR system are shown in Table 2.

Table 2: Galion LiDAR system specifications

Measurement range	75–1005 m
Spatial resolution	30 m
Accuracy	0.1 m/s
Wind speed range	0–70 m/s
Sampling time between two scans	3.4 s
Laser elevation angles	3°–75° evenly spaced by 3°

In this study, two-dimensional vertical scans of the wind field were performed by varying the elevation angle of the laser while keeping the azimuthal angle fixed (RHI scans). By setting the azimuthal angle on the direction of the centre of the turbine, two-dimensional measurements using the LiDAR were conducted over the vertical symmetry plane of the wind turbine wake. The LiDAR was located 185 m west from the turbine (Figure 1). The test was performed with 25 different laser elevation angles evenly spaced by 3°. Each vertical scan required approximately 85 s. The horizontal wind speed was calculated by assuming the negligible vertical wind speed and the wind direction from the supervisory control and data acquisition (SCADA) data.

3. Main body of abstract

3.1 Wind condition on the field test site

The SCADA data of the tested wind turbine for the testing period include the wind speed at hub height from an anemometer mounted on the nacelle, the nacelle yaw angle, the rotational speed of the wind turbine rotor, and the generated power. A histogram of the mean wind speed obtained from SCADA data is shown in Figure 2. The figure shows that wind speeds between 3 and 8 m/s were the primary speeds in the test site during the testing period. A wind rose evaluated using the SCADA data is shown in Figure 3. The figure shows that major wind directions during the testing period were ESE and WSW. A histogram of the mean tip speed ratio obtained from the SCADA data is shown Figure 4. The relationship between the power coefficient, C_P, (=$2P/\rho\pi R^2 U_\infty^3$, where P is the generated power, ρ is the air density, R is rotor radius and U_∞ is nacelle wind speed) and tip speed ratio, λ, are shown in Figure 5.

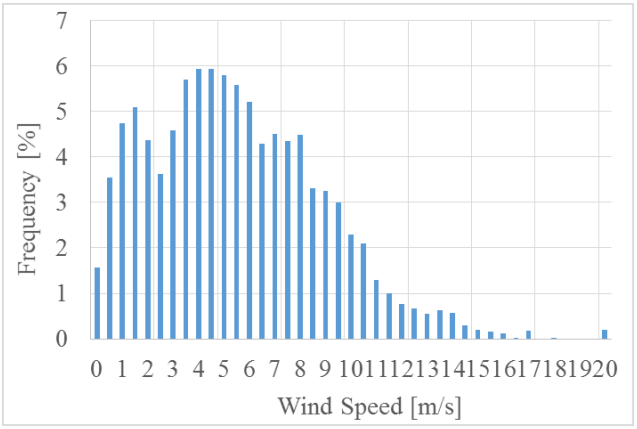

Figure 2: Histogram of the mean wind speed obtained from SCADA data during the testing period with a sampling time of 10 min

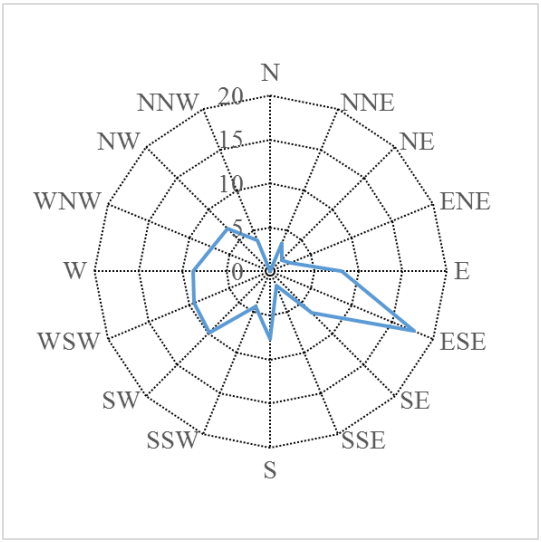

Figure 3: Wind rose evaluated using the SCADA data during the testing period

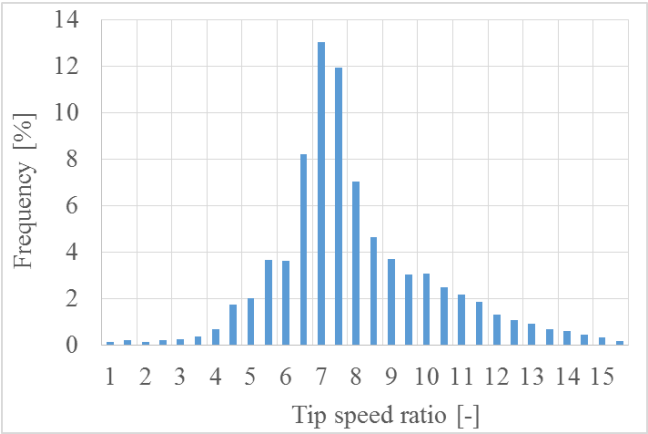

Figure 4: Histograms of the mean tip speed ratio obtained from SCADA data during the testing period with a sampling time of 10 min

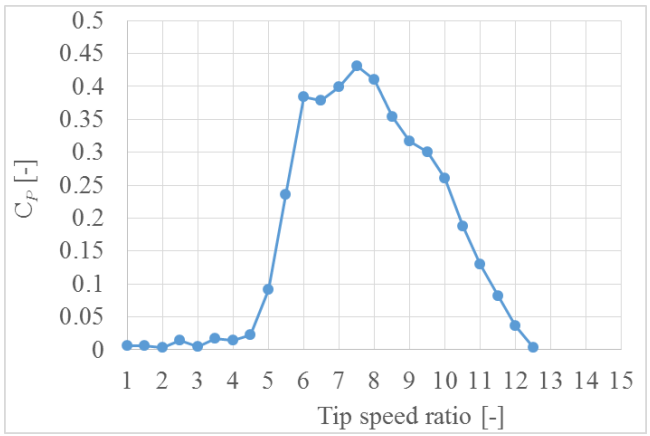

Figure 5: Power coefficient versus tip speed ratio evaluated from the SCADA data for the testing period

3.2 Experimental results

The positions of the wake profiles obtained using the LiDAR are shown in Figure 6, where D is the rotor diameter.

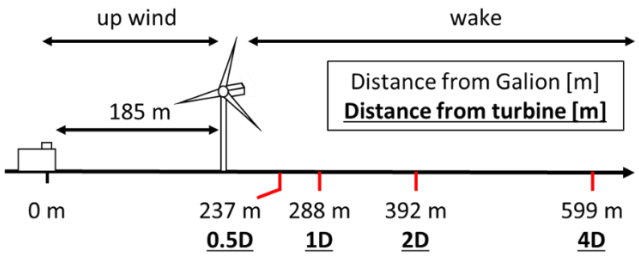

Figure 6: Positions of wake profiles obtained using the LiDAR

The vertical wake profiles of the mean normalized horizontal wind speed at low and high tip speed ratios are shown in Figures 7 and 8, respectively. The wind speed is normalized with the inflow horizontal wind speed obtained using the LiDAR. The tip speed ratios are calculated using the wind speed obtained from the SCADA data. The tip speed ratios between 5.5 and 7 are defined as the low ones and the ratios greater than 9 are defined as the high ones. The red lines in Figures 7 and 8 indicate the range of the wind turbine rotor.

Both Figures 7 and 8 show that there are strong velocity reductions and a steep velocity gradient near the rotor tip at both tip speed ratios. This trend is stronger at high tip speed ratios. The velocity reduction is small near the rotor centre and smaller at higher tip speed ratios. These observations trends are similar to the results of a wind tunnel test in a previous study [7].

However, Figures 7 and 8 indicate that downstream recovery of the velocity deficit is more rapid at low tip speed ratios. This observation is dissimilar to a result of the previous wind tunnel study that the recovery of the velocity deficit is relatively more rapid than the optimum up to 4D from the wind turbine at high tip speed ratios because of strong velocity gradients. This dissimilarity can be caused by fluctuation of the wind direction and the atmospheric boundary layer. In addition, this dissimilarity can be caused by changes in both the turbine rotational speed and wind velocity, whereas the upwind velocity and the wind direction are constant in the previous wind tunnel test.

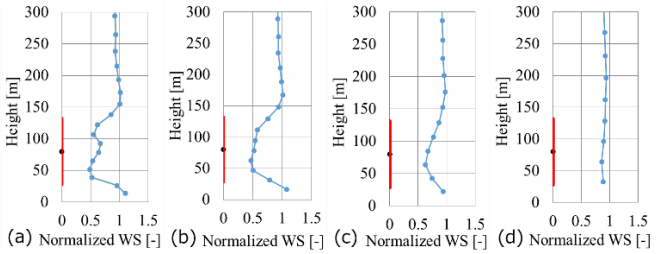

Figure 7: Vertical wake profiles of the mean normalized horizontal wind speed at low tip speed ratios ($5.5 \leq \lambda \leq 7$) Downwind distance from the turbine (a) 0.5D (b) 1D (c) 2D (d) 4D

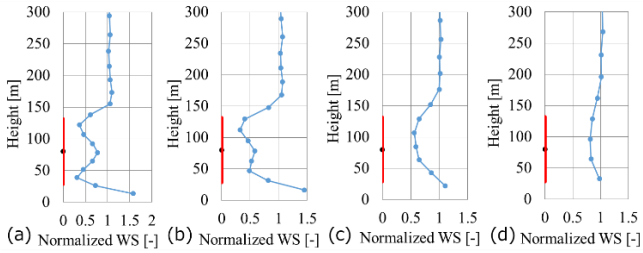

Figure 8: Vertical wake profiles of the mean normalized horizontal wind speed at high tip speed ratios ($\lambda \geq 9$)
Downwind distance from the turbine (a) 0.5D (b) 1D (c) 2D (d) 4D

4. Conclusion

We performed wind turbine wake measurements using a Galion LiDAR at a flat terrain site in Japan and examined the influence of tip speed ratio on the wind turbine wake property. The obtained results are follows:

・There are strong velocity reductions and a steep velocity gradient near the rotor tip and weak velocity reductions near the rotor centre. These trends are stronger at high tip speed ratios and are similar to the results of a previous wind tunnel test.

・Downstream recovery of the velocity deficit is more rapid at low tip speed ratios. This trend is dissimilar to the result of the previous wind tunnel test. This dissimilarity can be the result of the wake easily mixing with freestream because of the fluctuation in the wind direction and the atmospheric boundary layer, unlike the behaviour in the wind tunnel tests.

5. Learning objectives

In this paper, we investigated the influence of tip speed ratio on the wind turbine wake property using a Galion LiDAR in order to store field test data for the development of a general wake model, including the influences of wind turbine operation. We achieved benchmark field test data at a flat terrain wind turbine site, which is the most basic site. We will conduct wake measurements using the LiDAR at complex terrain wind turbine sites and study the influence of terrain configuration on wake property.

We will also conduct wake measurements using the LiDAR

operating yaw angle of a wind turbine and study the effect of yaw angle on wake property.

Acknowledgments

I acknowledge Electric Power Development Co., Ltd., The Japan Steel Works, Ltd. and Japan Meteorological Corporation for their support in obtaining the wind, turbine and LiDAR data measurements.

References

[1] L. J. Vermeer, J. N. Sørensen, and A. Crespo, "Wind turbine wake aerodynamics," *Prog. Aerosp. Sci.*, vol. 39, pp. 467–510, 2003.

[2] W. Tian, A. Ozbay, and H. Hu, "Effects of incoming surface wind conditions on the wake characteristics and dynamic wind loads acting on a wind turbine model," *Phys. Fluids*, vol. 26, no. 12, 2014.

[3] M. Bastankhah and F. Porté-Agel, "A wind-tunnel investigation of wind-turbine wakes in yawed conditions," *J. Phys. Conf. Ser.*, vol. 625, no. 1, 2015.

[4] Y. Kamada, J. Murata, T. Maeda, T. Ito, A. Okawa, S. Yonekura, and T. Kogaki, "Experimental Study on Wind Turbine Wake and Rotor Output in Wake with Various Turbulence Intensity," *Turbomachinery*, vol. 40, no. 2, pp. 97–103, 2012.

[5] T. Maeda, Y. Kinpara, and T. Kakinaga, "Wind Tunnel and Field Experiments on Wake Behind Horizontal Axial Wind Turbine," *Trans. JSME*, vol. 71, no. 701, pp. 162–170, 2005.

[6] B. Andresen, "Wake behind a wind turbine operating in yaw," *Nor. Univ. Sci. Technol.*, vol. Master of, 2013.

[7] P. Å. Krogstad and M. S. Adaramola, "Performance and near wake measurements of a model horizontal axis wind turbine," *Wind Energy*, vol. 15, pp. 743–756, 2012.

[8] G. More and D. Gallacher, "Lidar Measurements and Visualisation of Turbulence and Wake Decay Length," *EWEA*, 2014.

[9] G. V. Iungo, Y.-T. Wu, and F. Porté-Agel, "Field Measurements of Wind Turbine Wakes with Lidars," *J. Atmos. Ocean. Technol.*, vol. 30, no. 2, pp. 274–287, 2013.